AGU PUBLICATIONS

Geophysical Research Letters

RESEARCH LETTER
10.1002/2017GL073933

Key Points:
- Substantial uptake of oxygen is observed in the Labrador Sea during the 2014–2015 winter
- Stronger oxygen sink compared to previous studies is linked to North Atlantic Oscillation
- Many commonly used gas exchange parameterizations underestimate the observed flux dramatically

Supporting Information:
- Supporting Information S1

Correspondence to:
J. Koelling,
jkoelling@ucsd.edu

Citation:
Koelling, J., D. W. R. Wallace, U. Send, and J. Karstensen (2017), Intense oceanic uptake of oxygen during 2014–2015 winter convection in the Labrador Sea, *Geophys. Res. Lett.*, *44*, doi:10.1002/2017GL073933.

Received 22 APR 2017
Accepted 14 JUL 2017
Accepted article online 19 JUL 2017

Intense oceanic uptake of oxygen during 2014–2015 winter convection in the Labrador Sea

Jannes Koelling[1], Douglas W. R. Wallace[2], Uwe Send[1], and Johannes Karstensen[3]

[1]Scripps Institution of Oceanography, La Jolla, California, USA, [2]Department of Oceanography, Dalhousie University, Halifax, Nova Scotia, Canada, [3]GEOMAR Helmholtz Centre for Ocean Research Kiel, Kiel, Germany

Abstract Measurements of near-surface oxygen (O_2) concentrations and mixed layer depth from the K1 mooring in the central Labrador Sea are used to calculate the change in column-integrated (0–1700 m) O_2 content over the deep convection winter 2014/2015. During the mixed layer deepening period, November 2014 to April 2015, the oxygen content increased by 24.3 ± 3.4 mol m^{-2}, 40% higher than previous results from winters with weaker convection. By estimating the contribution of respiration and lateral transport on the oxygen budget, the cumulative air-sea gas exchange is derived. The O_2 uptake of 29.1 ± 3.8 mol m^{-2}, driven by persistent undersaturation (≥ 5%) and strong atmospheric forcing, is substantially higher than predicted by standard (nonbubble) gas exchange parameterizations, whereas most bubble-resolving parameterizations predict higher uptake, comparable to our results. Generally large but varying mixed layer depths and strong heat and momentum fluxes make the Labrador Sea an ideal test bed for process studies aimed at improving gas exchange parameterizations.

1. Introduction

The Labrador Sea is one of the few regions where open-ocean deep convection occurs [*Marshall and Schott*, 1999], with Labrador Sea Water (LSW) forming in the interior of the basin [*Lazier*, 1973; *Clarke and Gascard*, 1983] and spreading throughout the Atlantic as part of North Atlantic Deep Water (NADW) [*Talley and McCartney*, 1982]. In the LSW formation process, vertical mixing and temperature-driven solubility changes outpace the uptake of atmospheric oxygen by air-sea gas transfer [*Ito et al.*, 2004], resulting in newly formed LSW being about 6% undersaturated relative to equilibrium [*Clarke and Coote*, 1988]. This marked air-sea disequilibrium, along with strong winds, makes the Labrador Sea one of the most intense sinks of atmospheric oxygen in the world ocean [*McKinley et al.*, 2003]. NADW exports oxygen to the ocean interior, where it plays an important role in supporting respiration and biogeochemical cycling of nutrients and carbon [*Keeling et al.*, 2010]. A recent study on changes in the global oxygen content since the 1960s [*Schmidtko et al.*, 2017] found that the amount of oxygen stored in the deep ocean decreased by 702.9±244 Tmol per decade and suggested that changes in ventilation at high latitudes may have contributed to this decline.

Considering the importance of LSW for the transfer of oxygen from the atmosphere to the global deep ocean, and given the climate sensitivity of its formation [*Curry et al.*, 1998], it is crucial to understand the processes governing variability of air-sea gas exchange in this region. While oxygen data have been collected regularly during hydrographic cruises in the region [*Stendardo and Gruber*, 2012], there have been relatively few attempts to directly measure the uptake of oxygen during the convection season, including one study of oxygen content changes in 2003–2004 from Argo float data [*Körtzinger et al.*, 2004] and a previous mooring-based study focusing on seasonal cycles of carbon and oxygen in the mixed layer [*Körtzinger et al.*, 2008]. The aim of this study is to quantify the total uptake of oxygen between November 2014 and April 2015, a period featuring the deepest convection since 1994 [*Yashayaev and Loder*, 2016], and compare it to these earlier estimates and to the uptake predicted by several widely used air-sea gas exchange parameterizations.

2. Data and Methods

2.1. Data

Observational data used in this study come from the K1 mooring, which is located in the LSW formation region (Figure 1) and has been continuously measuring temperature and salinity throughout the water column since the early 1990s [*Avsic et al.*, 2006]. The three uppermost instruments additionally collected oxygen

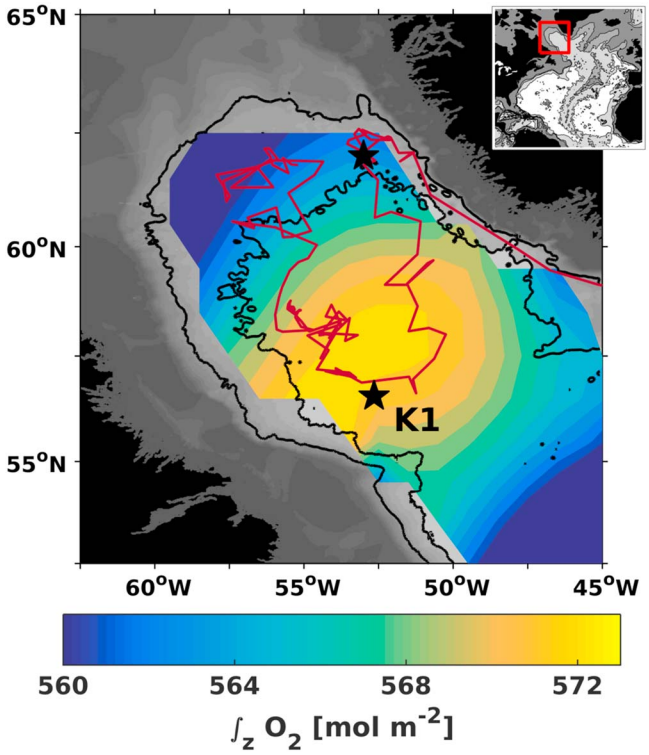

Figure 1. Map of the Labrador Sea, with topography as gray background shading, and 2000 m and 3000 m isobaths as black lines; colors show 100–2000 m O_2 content from the World Ocean Database [*Levitus et al.*, 2013], red line shows track of Argo float used to estimate F_{lat} (section 2.2), and locations of K1 and the eddy formation region are shown as black symbols. Inset shows the location of the study area within the North Atlantic.

data for the K1 deployment KPO 1117 analyzed here, using a Seabird Microcat model 43 [*Carlson*, 2002] at depths of 10 m and 100 m and an Aanderaa Optode model 4835 [*Tengberg et al.*, 2006] at 60 m. The mooring was deployed from August 2014 to May 2016; however, none of the oxygen sensors returned data after May 2015, as all three instruments were either lost or ran out of battery power, limiting our study to the 2014–2015 winter. All instruments were new and calibrated by their respective manufacturers prior to deployment, but a postcalibration of the oxygen sensors was impossible due to the sensor failures outlined above. While both types of sensors have been shown to be susceptible to drift [*D'Asaro and McNeil*, 2013], we find good agreement between the instruments after December 2014, differing only by a constant offset (Figure S1 in the supporting information), with no signs of a trend in the differences which would be expected in the case of instrument drift. We adjust for this offset by matching their values when all three sensors were in the mixed layer and additionally correct for sensor drift that can occur during storage between the factory calibration and deployment [*Bittig et al.*, 2012] by comparing data collected during the first 15 days of measurements to a conductivity-temperature-depth (CTD) profile taken at the site prior to deployment, adding an offset of 11.25 ± 2 μmol L^{-1} to the mooring data to agree with CTD measurements (Figure S2).

2.2. Oxygen Budget

To calculate the change in column-integrated 0–1700 m O_2 content, we combine time series of surface oxygen concentration and mixed layer depth (MLD). For surface data, we use 6-hourly telemetered data from the 10 m instrument, interpolated onto a 1 h time grid, until December 2014, and 1-hourly measurements from the 60 m instrument afterward, when the mixed layer was generally at least several hundred meters deep. Surface concentration and saturation, as well as MLD, estimated using a criterion of $\Delta\sigma_\theta \leq 0.01$ kg m^{-3}, and contours of $O_2(z, t_n)$ (see below), are shown in Figure 2.

Oxygen concentrations throughout the water column are estimated by an iterative procedure, starting with a profile $O_2(z, t_0)$, taken from a nearby CTD cast, as the initial condition, and setting O_2 within the mixed layer

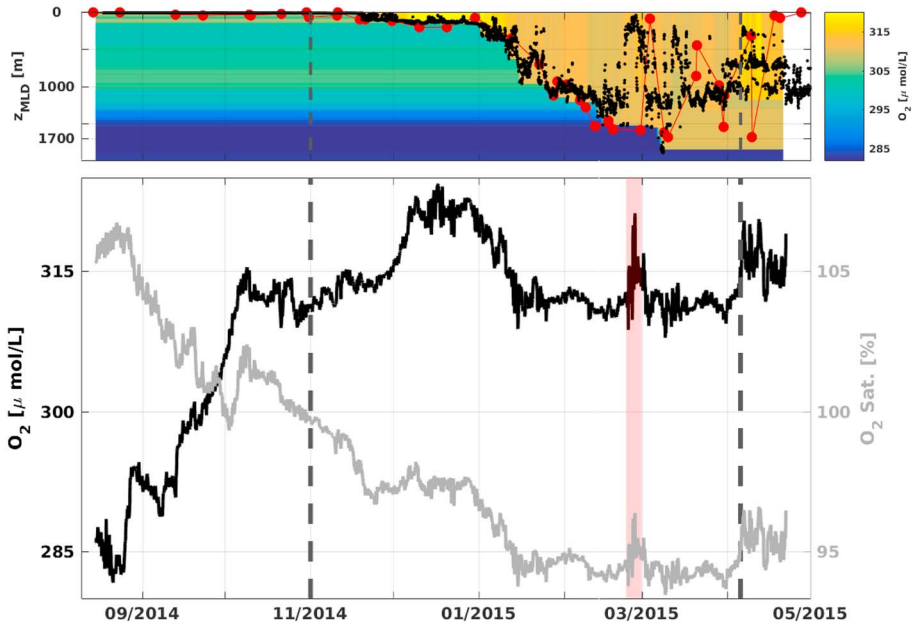

Figure 2. (top) Daily mean mixed layer depth, z_{MLD} from mooring data (black dots), instantaneous z_{MLD} from Argo profiles within 100 km of the K1 site (red circles), and contours of $O_2(z, t)$, calculated from equation (1). (bottom) Surface oxygen concentration (black) and saturation (gray). Red shading marks the passing of an eddy, and dashed vertical lines show the start and end times for the analysis of gas exchange (Figure 3).

to surface values for each time step, such that

$$\begin{aligned} O_2(z, t_n) &= O_{2_{surf}} \qquad z \le z_{mld}(t_n) \\ O_2(z, t_n) &= O_2(z, t_{n-1}) \qquad z > z_{mld}(t_n) \end{aligned} \tag{1}$$

where $O_{2_{surf}}$ is the surface oxygen concentration, $z_{mld}(t_n)$ is the mixed layer depth at time t_n, and the oxygen content is calculated as the vertical integral of $O_2(z, t_n)$. This method assumes that oxygen concentrations are constant throughout the mixed layer during convection, which has been shown to be the case with Argo float data [*Körtzinger et al.*, 2004]. We further tested this approach with temperature data, comparing heat content estimated from surface temperature and MLD to that calculated using all mixed layer temperature data, and found good agreement (Figure S3).

The change in oxygen content is the sum of the fluxes due to gas exchange (F_{gasex}), biological activity (F_{bio}), and lateral exchange through transport processes from outside the convection region (F_{lat}):

$$\int_z O_2(z, t_n) - \int_z O_2(z, t_{n-1}) = \left(F_{gasex} + F_{bio} + F_{lat}\right)\Delta t \tag{2}$$

F_{gasex} can thus be calculated from the measured oxygen content changes, along with estimates of F_{bio} and F_{lat}. Previous studies have shown that there is heat transport from the boundary current west of Greenland into the central basin, caused by southward propagation of Irminger Current eddies [*Straneo*, 2006; *Yashayaev and Loder*, 2009; *de Jong et al.*, 2016]. This can be used to estimate an associated eddy-driven flux of oxygen:

$$F_{lat} = F^H_{lat} \frac{\Delta \int_z O_2}{\Delta \int_z T c_p \rho} \tag{3}$$

where F^H_{lat} is the lateral heat flux inferred from mooring and North American Regional Reanalysis (NARR) data and $\frac{\Delta \int_z O_2}{\Delta \int_z T c_p \rho}$ is the ratio of the mean oxygen to heat content gradients between K1 and the eddy formation region at the spreading point of the 2000 m and 3000 m isobaths [*Lilly et al.*, 2003], calculated to be -2.84 ± 0.59 mol $(GJ)^{-1}$ from Argo data. With $F^H_{lat} = 1.01 \pm 0.5$ GJ m^{-2}, equation (3) yields $F_{lat} = -2.9 \pm 1.5$ mol m^{-2}; see Text S1 for details on the calculation of F^H_{lat} and $\frac{\Delta \int_z O_2}{\Delta \int_z T c_p \rho}$.

We assume a net heterotrophic ocean due to light limitation in winter inhibiting production [*Harrison and Li*, 2007]. A previous study at the K1 site by *Körtzinger et al.* [2008] used measurements of dissolved inorganic

Table 1. Components of the Oxygen Budget (Equation (2)), and Gas Exchange Estimated From Different Parameterizations Using NARR Wind Speed Data, Integrated From November to April[a]

Parameter	Reference	O_2 (mol m^{-2})	Difference (%)
0–1700 m inventory change ($\Delta \int_z O_2$)	This study	24.3 ± 3.4	
Lateral transport (F_{lat})	This study	-2.9 ± 1.5	
Biological activity (F_{bio})	*Körtzinger et al.* [2008]	-1.9 ± 0.7	
Total gas exchange	This study	29.1 ± 3.8	
F_s	*Wanninkhof* [2014] (W14)	9.2 ± 2.1	−69
F_s	*Wanninkhof* [1992] (W92)	11.4 ± 2.6	−61
F_s	*Kihm and Körtzinger* [2010] (KK10)	14.9 ± 3.6	−49
$F_s + F_p$	*Woolf and Thorpe* [1991] (WT91)	10.6 ± 1.2	−64
$F_s + F_p + F_c$	*Liang et al.* [2013] (L13)	19.8 ± 2.4	−32
$F_s + F_p$	*Woolf* [1997] (W97)	28.8 ± 3.1	−1
$F_s + F_p + F_c$	*Stanley et al.* [2009] (S09)	31.5 ± 2.6	+8
$F_s + F_c$	*Vagle et al.* [2010] (V10)	38.2 ± 3.2	+31

[a]The terms included in the parameterizations are given in the left column; F_s: diffusive gas exchange; F_p: partially dissolving bubbles; F_c: completely dissolving bubbles.

carbon to estimate that 40% of summertime net community production, amounting to 1.4 ± 0.5 mol C m^{-2}, is remineralized above the base of the winter mixed layer, while the remaining 60% is exported below the depth of convection. Using a stoichiometric ratio of −1.34 O_2:C [*Körtzinger et al.*, 2001], this corresponds to an integrated wintertime flux of -1.9 ± 0.7 mol O_2 m^{-2}, which we use as an estimate of F_{bio} in this study.

2.3. Air-Sea Gas Exchange Parameterizations

Several parameterizations for air-sea gas exchange are used to estimate the time-varying gas transfer from the measured surface data, along with wind speed from satellite and atmospheric reanalysis data. All parameterizations involve some measure of the piston velocity k_{660} that is dependent on wind speed:

$$k_{660} = a(U_{10})^n \tag{4}$$

where U_{10} is the wind speed measured at 10 m in the atmosphere, the exponent n is typically chosen as either 2 [*Wanninkhof*, 1992, 2014] or 3 [*Wanninkhof and McGillis*, 1999; *Kihm and Körtzinger*, 2010], and a is an empirically derived constant. k_{660} refers to the piston velocity at a Schmidt number of 660 [*Wanninkhof*, 2014], which corresponds to CO_2 at 20°C, with the piston velocity for any other gas given by $k = k_{660}(\frac{Sc}{660})^{-0.5}$. The diffusive air-sea flux for oxygen is proportional to the difference in the surface concentration, O_2^{sea}, from the equilibrium concentration, O_2^{sat}, and is given by

$$F_s = k_{O_2}(O_2^{sat} - O_2^{sea}) \tag{5}$$

with positive values denoting oceanic oxygen uptake. Many commonly used gas exchange parameterizations [*Wanninkhof*, 1992, 2014; *Kihm and Körtzinger*, 2010] assume that the total flux of a gas can be described by equations (4) and (5), with $F_{gasex} = F_s$, and use an a priori choice of n and measurements or estimates of all other parameters to find a best fit for a.

However, particularly for less soluble gases and at high wind speeds, there is also an important contribution from air injection, and the flux is more accurately represented by $F_{gasex} = F_s + F_p + F_c$ [*Liang et al.*, 2013], with F_p and F_c referring to the flux from partially and completely dissolving bubbles, respectively. F_p, like F_s, depends on wind speed and concentration difference but has an additional term accounting for the hydrostatic pressure in large bubbles; F_c depends only on the wind speed and the atmospheric mole fraction of the respective gas, χ [*Emerson and Bushinsky*, 2016]. The gas exchange parameterizations with bubble terms used in this study are those of *Woolf and Thorpe* [1991], *Woolf* [1997], *Stanley et al.* [2009], *Vagle et al.* [2010], and *Liang et al.* [2013]. The inverse method used in *Vagle et al.* [2010] to parameterize gas exchange only includes data for $U_{10} > 12$ m s^{-1} and is therefore poorly constrained below this threshold; we complement their parameterization by using the relationship of *Woolf and Thorpe* [1991] for $U_{10} \leq 12$ m s^{-1}.

Oxygen solubility is calculated from the equations of *Garcia and Gordon* [1992], and corrected for pressure effects following *Benson and Krause* [1984], using barometric pressure from the Fleet Numerical Meteorology

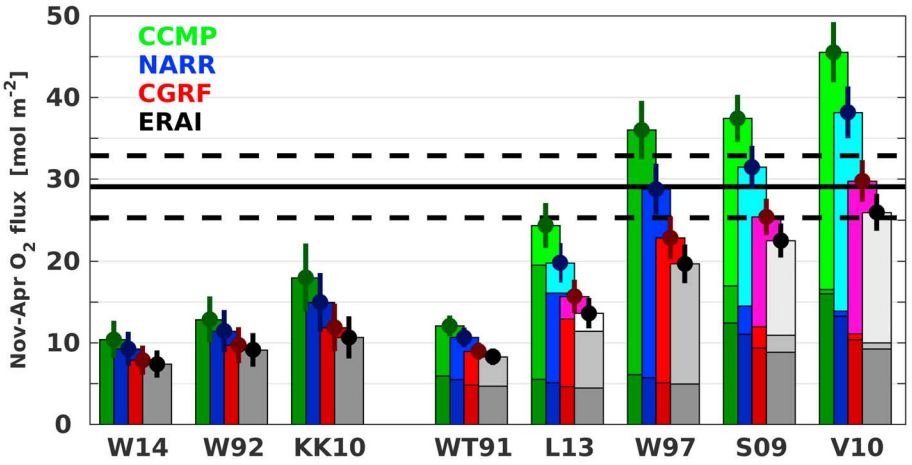

Figure 3. Horizontal lines show cumulative (November–April) uptake of oxygen at K1, calculated from equation (2), with confidence interval. Bars and symbols show the analogous November–April O_2 uptake calculated from different parameterizations. Colors correspond to different wind speed products, and the shading of the bars shows contributions of F_s (darkest), F_p (intermediate), and F_c (lightest). Abbreviations are defined in Table 1; a gap separates parameterizations with and without bubbles.

and Oceanography Center (FNMOC) product. For wind speed, we use data from the cross-calibrated multiplatform (CCMP) product [*Atlas et al.*, 2011], European Centre for Medium-Range Weather Forecasts ERA-Interim (ERAI) [*Dee et al.*, 2011], the National Centers for Environmental Prediction (NCEP) North American Regional Reanalysis (NARR) [*Mesinger et al.*, 2006], and CMC GDPS reforecasts (CGRF) [*Smith et al.*, 2014]. Wind speed data from NARR compare most favorably with observations in the Irminger Sea and off Cape Farewell [*Moore et al.*, 2008; *Renfrew et al.*, 2009], with a slope of 0.99 between observational and reanalysis data and a bias of −1.5 m s^{-1}, reported by *Renfrew et al.* [2009]. NARR data are corrected for this bias and used to calculate the gas exchange estimates shown in Table 1, and results based on data from all products are compared in Figure 3. The data were interpolated from their native 6-hourly (FNMOC, CCMP, and ERAI), 3-hourly (NARR), or 1-hourly (CGRF) resolution onto the 1-hourly time grid used in this study.

3. Results

Surface concentration and saturation of oxygen, along with MLD, are shown in Figure 2; the concentration rapidly increased in early December to peak values of ~320 μ mol L^{-1} (~97% saturation), as the mixed layer was still relatively shallow and some of the strongest winds in our records (Figure S4) drove increased uptake, then dropped to around 310 μ mol L^{-1} at 95% saturation in early January, when the mixed layer started deepening at a higher rate, and continued to decrease slightly throughout the rest of winter. MLD calculated from the mooring data agrees well with individual Argo profiles taken within 100 km of the mooring before early April, after which the mixed layer shoaled to a depth shallower than the uppermost available measurements, resulting in mooring data overestimating z_{MLD}. We therefore limit our analysis of gas exchange to the period from 1 November, when oxygen saturation dropped below 100%, to 5 April, marking the last time step for which the shallowest measurement is within the mixed layer.

The difference in oxygen content between 1 November and 5 April, calculated from equation (1), is 24.3 ± 3.4 mol m^{-2}. For the same time period, F_{lat} is calculated to be −2.9 ± 1.5 mol m^{-2} using equation (3) and F_{bio} is estimated as −1.9 ± 0.7 mol m^{-2} (see section 2.2). The resulting estimate for air-sea gas exchange in the Labrador Sea during the 2014–2015 winter, calculated from equation (2), is 29.1 ± 3.8 mol m^{-2} and is compared with the cumulative gas exchange estimates predicted by different parameterizations in Figure 3; the results are also summarized in Table 1.

All gas exchange parameterizations including only an F_s term (equation (5)) underestimate the uptake of oxygen over the convection season by 49% or more using NARR winds; additional such parameterizations not shown here [e.g., *Liss and Merlivat*, 1986; *Nightingale et al.*, 2000; *Sweeney et al.*, 2007; *Wanninkhof et al.*, 2009] generally fall below that of *Wanninkhof* [1992] at high wind speeds [*Körtzinger et al.*, 2008] and will

therefore similarly predict a lower flux than observed. With the exception of *Woolf and Thorpe* [1991], the bubble-resolving parameterizations predict a greater uptake than the purely diffusive ones, but there is considerable variability between them, with estimates ranging from 19.8 ± 2.4 mol m^{-2} [*Liang et al.*, 2013] to 38.2 ± 3.2 mol m^{-2} [*Vagle et al.*, 2010]. Two parameterizations, *Woolf* [1997] and *Stanley et al.* [2009], agree within the error with the observed gas exchange, at 28.8 ± 3.1 mol m^{-2} and 31.5 ± 2.6 mol m^{-2}.

4. Discussion

4.1. Observed Change

The 0–1700 m depth range used to calculate the oxygen content is chosen to reflect conditions typical of the entire central Labrador Sea, as *Yashayaev and Loder* [2016] determined 1700 m to be the aggregate depth of convection during that winter. Our data show that the water column at the mooring site was homogenized to more than 1800 m during an event in March lasting several days, reaching a maximum of 1850 m on 8 March (Figure 2). However, Argo profiles taken within 100 km of the mooring show no evidence of convection reaching below 1700 m, suggesting that this was a small-scale feature, such as a convective plume [*Marshall and Schott*, 1999] or passing cold-core eddy [*Avsic et al.*, 2006], and we do not expect these deeper mixed layers to be representative of the whole region.

The change in 0–1700 m oxygen content observed between 1 November and 5 April is 24.3 ± 3.4 mol m^{-2}, 40% higher than the increase of 17 mol m^{-2} observed by *Körtzinger et al.* [2004] over a comparable time period in the 2003/2004 winter, when convection reached about 1400 m. *Stendardo and Gruber* [2012] found evidence for a connection between oxygen content in the deep North Atlantic and variability related to the North Atlantic Oscillation (NAO), and data from biogeochemical models suggest that Labrador Sea oxygen uptake is strongest during the positive phase of the NAO [*McKinley et al.*, 2003], which is associated with both higher wind speeds and stronger surface heat loss in the Labrador Sea [*Hurrell et al.*, 2013], resulting in generally deeper convection [*Curry et al.*, 1998; *Yashayaev and Loder*, 2016]. The NAO was positive in 2014–2015 and weakly negative during the 2003–2004 period of *Körtzinger et al.* [2004], consistent with these earlier results. The oxygen content change we observe in the upper 1400 m is 16.3 ± 2.8 mol m^{-2}, in good agreement with *Körtzinger et al.*'s [2004] estimate, which could suggest that the higher uptake of oxygen in 2014–2015 is caused by convection penetrating to greater depth, enhancing upward mixing of low-saturation deep waters. However, the increased wind forcing and solubility pump during positive NAO years would also be expected to increase the flux of O_2, and more sustained observations will be necessary to better understand the mechanisms responsible for the link between the NAO and oxygen uptake.

Assuming that our results are representative of the whole convection region, with an approximate area of 100,000 km^2, the difference in oxygen content change between a positive (2014–2015) and neutral (2003–2004) NAO winter, 7.3 ± 3.4 mol m^{-2}, corresponds to about 0.73 ± 0.34 Tmol $(yr)^{-1}$, only 1% of the global loss of 702.9 ± 244 Tmol $(decade)^{-1}$ (= 70.3 ± 24.4 Tmol $(yr)^{-1}$) reported by *Schmidtko et al.* [2017], suggesting that changes in air-sea gas exchange in the Labrador Sea alone are unlikely to have played a major role in the decline of the oceanic oxygen content in recent decades. However, the effect of LSW on the global circulation [*Jackson et al.*, 2016] and interannual variability in its export [*Yashayaev and Loder*, 2016] also plays a role in controlling ventilation of the deep ocean and will need to be more thoroughly studied to fully understand its impact on the global oxygen budget.

4.2. Gas Exchange Parameterizations

While the importance of bubbles in air-sea gas exchange has been emphasized for some time [*Thorpe*, 1982; *Woolf and Thorpe*, 1991; *Wallace and Wirick*, 1992; *Keeling*, 1993], parameterizations that do not account for their effect are still widely used. Many such parameterizations were derived for CO_2, which is more soluble than oxygen and therefore less affected by bubble processes [*Woolf and Thorpe*, 1991; *Liang et al.*, 2013], but are assumed to hold for other gases if scaled by the Schmidt number. As shown in Figure 3, neglecting bubble process is not appropriate for oxygen in the Labrador Sea, with the parameterizations of *Wanninkhof* [1992, 2014] and *Kihm and Körtzinger* [2010] underestimating the observed uptake by 49–69% when calculated with NARR wind data. In addition to being used in observational studies, many of the models included in the Climate Model Intercomparison Project (CMIP5) [*Taylor et al.*, 2012] also utilize the parameterization of *Wanninkhof* [1992], or a slight variation thereof, to compute air-sea gas exchange of O_2, CO_2, and other gases [*Weaver et al.*, 2001; *Tjiputra et al.*, 2010; *Dufresne et al.*, 2013; *Dunne et al.*, 2013; *Ilyina et al.*, 2013]. Considering

the large discrepancy between our results and the flux predicted from the *Wanninkhof* [1992] parameterization, we expect these global models to underestimate the strength of oxygen sinks at high latitudes, where strong winds and bubble injection are most prevalent.

Despite accounting for bubbles, both the *Woolf and Thorpe* [1991] and *Liang et al.* [2013] parameterizations underestimate the uptake, by around 60% and 30%, respectively. In contrast, recent studies on noble gas supersaturation [*Emerson and Bushinsky*, 2016] and on O_2 uptake in relation to net community production [*Plant et al.*, 2016] in the Pacific Ocean found that *Liang et al.* [2013] provided the best fit to their data. The poorer performance of *Liang et al.* [2013] in the present study is likely related to the lower surface saturation and stronger physical forcing in the form of winds, wave breaking, and convection and could reflect either real regional variability in bubble processes or shortcomings of the parameterization in accurately predicting them in conditions typical of the Labrador Sea.

All other bubble-resolving parameterizations predict considerably higher uptake, closer to the observed gas exchange. While the parameterizations of *Woolf* [1997] and *Stanley et al.* [2009] agree within uncertainty bounds with the observed cumulative gas exchange, the estimate from the parameterization of *Vagle et al.* [2010] is 30% higher than the observed uptake when calculated with NARR wind speed data. However, *Vagle et al.*'s [2010] relationships between wind speed, bubble penetration depth, and gas exchange were derived using wind data from the NCEP/NCAR (National Center for Atmospheric Research) reanalysis [*Kalnay et al.*, 1996], which are biased low relative to NARR [*Renfrew et al.*, 2009]; recalculating the gas exchange with the NCEP product yields an estimate of 30.5 $\pm$ 2.6 mol m^{-2}, matching the observed uptake. This difference of almost 30% illustrates the high sensitivity to the choice of wind speed product (see also Figure 3), with discrepancies between products resulting in biases that need to be accounted for when using parameterizations to estimate gas exchange in budget calculations. Our assessment that bubble terms are necessary to accurately determine the flux of oxygen at high latitudes is not dependent on which of the common wind speed products we use, and possible biases are too small to alter our conclusion: some of the products used here have been shown to have biases up to 3 m s^{-1} at high (>20 m s^{-1}) wind speeds [*Renfrew et al.*, 2009; *Li et al.*, 2013], but only 2.5% of the NARR data at K1 are above this threshold. Even if a bias underestimating the winds was present for a broader wind speed range (e.g., $U_{10} > 15$ m s^{-1}), it would have to exceed 13 m s^{-1} [*Wanninkhof*, 1992], 19 m s^{-1} [*Wanninkhof*, 2014], or 5 m s^{-1} [*Kihm and Körtzinger*, 2010] for these nonbubble parameterizations to agree within the error with the observed cumulative oxygen uptake.

An additional source of uncertainty are the assumptions underlying our estimates of F_{bio} and F_{lat}, which are difficult to validate given the sparsity of relevant data from the region. For F_{bio}, previous studies have shown that there is almost no primary production during winter in the Labrador basin [*Harrison and Li*, 2007; *Harrison et al.*, 2013; *Körtzinger et al.*, 2008], suggesting net heterotrophic conditions with $F_{bio} \leq 0$. Since K1 is situated within the region of maximum oxygen content (Figure 1), there cannot be a positive flux from mixing with waters from outside the central LS, such that $F_{lat} \leq 0$. This allows us to establish a lower bound for the estimated gas exchange, with $F_{bio} = F_{lat} = 0$. In this scenario, where $\Delta \int_z O_2 = F_{gasex}$, the nonbubble parameterizations still predict a lower gas exchange than we observe (Figure S6), showing that their low bias persists regardless of these assumptions. However, there is likely to be additional variability for both processes that cannot be resolved here; the amount of wintertime respiration is expected to vary with the strength of the preceding spring bloom, and seasonal or interannual variability may exist in the boundary-interior gradients of heat and O_2, affecting the magnitude of F_{lat}.

The parameterizations of *Stanley et al.* [2009], *Vagle et al.* [2010], and *Liang et al.* [2013] agree well in the relative strength of the diffusive and bubble flux, with 26% to 35% of the total flux coming from F_s, but the importance of the two bubble terms differs between the different models: F_p and F_c are responsible for 55% and 19% in *Liang et al.* [2013], 11% and 54% in *Stanley et al.* [2009], and 1.5% and 64% in *Vagle et al.* [2010]. These differences show that there is still considerable uncertainty not only regarding the strength of bubble-induced gas exchange but also about the underlying dynamics.

5. Outlook

Our results show that in situ measurements from moorings can be used to estimate the seasonal change in oxygen content, even with relatively sparse instrumentation. Measuring oxygen in locations like the Labrador Sea may prove to be an important tool for future gas exchange studies, with severe undersaturation

throughout the winter months resulting in a strong and persistent signal, which mitigates the effect of measurement uncertainty on estimates of transfer velocity. As an example, using flux measurements at 95% saturation to infer the transfer velocity, the range of estimates resulting from a ± 2 μmol L^{-1} offset in the sensor calibration is reduced by a factor of 7.7 compared to the same calculation at 99% saturation (see Text S2 for details).

Recent advances in the in situ calibration and correction of oxygen sensors on Argo floats [*Takeshita et al.*, 2013; *Uchida et al.*, 2008; *Bittig et al.*, 2014], along with the extension of the Argo-Oxygen program [*Gruber et al.*, 2010], will enable studies of the spatial and interannual variability of the Labrador Sea's oxygen content and help put our findings into a broader context. However, the poor temporal resolution of float data will be insufficient to resolve the intense fluxes of oxygen on short time scales that have been observed in moored measurements [*Wallace and Wirick*, 1992; *Vagle et al.*, 2010]. An ideal observing system of oxygen transfer in the Labrador Sea should include high-frequency measurements of inventory changes from moorings to provide information on fluxes occurring on these shorter time scales, complemented by the more extensive but lower frequency data from the Argo program.

6. Conclusion

The change in Labrador Sea oxygen content of 24.3 ± 3.4 mol m^{-2} during the 2014–2015 winter is more than 40% higher than the 17 mol m^{-2} observed in the 2003–2004 winter by *Körtzinger et al.* [2004]. We attribute this to more intense air-sea gas exchange caused by unusually deep convection (1700 m) [*Yashayaev and Loder*, 2016], and increased atmospheric forcing during the positive NAO phase, in agreement with earlier studies from hydrography and models [*Stendardo and Gruber*, 2012; *McKinley et al.*, 2003]. Wintertime oxygen uptake is calculated as 29.1 ± 3.8 mol m^{-2} from the measured O_2 content change and an estimated 4.8 ± 1.7 mol m^{-2} loss through lateral transport and respiration.

Gas exchange parameterizations including only an F_s term invariably predict a lower November–April integrated oxygen uptake than we observe, even in the lower limit of zero biological and lateral transport fluxes. The cumulative air-sea flux calculated from bubble-resolving models is generally higher, with three of the five parameterizations considered in this study predicting an uptake of oxygen similar to our estimate, showing that resolving the impact of bubbles is essential for accurate estimation of net air-sea gas fluxes, even when the ocean is strongly ($\geq$ 5%) undersaturated relative to the atmosphere. However, there is substantial variation between parameterizations both in magnitude and in the partitioning of the flux between the different bubble processes.

Studying wintertime gas transfer in the Labrador Sea can help uncover the processes controlling gas exchange under the extreme atmospheric forcing and strong undersaturation of mixed layer oxygen characteristic of high latitudes and elucidate similarities and differences to the typically milder conditions in the subtropical and tropical oceans.

Acknowledgments
The authors would like to thank Dariia Atamanchuk, Craig McNeil, Mitchell Wolf, and Roberta Hamme for their helpful discussions and advice. Canadian support was via the Canada Excellence Research Chair in Ocean Science and Technology and the NSERC-supported VITALS (Ventilation, Interactions and Transport Across the Labrador Sea) project. K1 is part of the OceanSITES mooring network. Analysis was supported by the BMBF RACE II project, by the European Union's Horizon 2020 research and innovation program under grant agreement 633211 (AtlantOS) and by European Union's Seventh Framework Program (FP7/2007-2013) under grant agreement 308299 (NACLIM). Mooring and hydrography data used in this study are available from the authors on request and will also be made available online by GEOMAR. CCMP version 2.0 vector wind analyses are produced by Remote Sensing Systems. Data are available at www.remss.com. NCEP Reanalysis data were provided by the NOAA/OAR/ESRL PSD, Boulder, Colorado, USA, from their Web site at http://www.esrl.noaa.gov/psd/. CGRF forcing fields are made available by Environment and Climate Change Canada. Argo data were collected and made freely available by the International Argo Program and the national programs that contribute to it (http://www.argo.ucsd.edu and http://argo.jcommops.org). The Argo Program is part of the Global Ocean Observing System.

References

Atlas, R., R. N. Hoffman, J. Ardizzone, S. M. Leidner, J. C. Jusem, D. K. Smith, and D. Gombos (2011), A cross-calibrated, multiplatform ocean surface wind velocity product for meteorological and oceanographic applications, *Bull. Am. Meteorol. Soc.*, *92*, 157–174, doi:10.1175/2010BAMS2946.1.

Avsic, T., J. Karstensen, U. Send, and J. Fischer (2006), Interannual variability of newly formed Labrador Sea Water from 1994 to 2005, *Geophys. Res. Lett.*, *33*, L21S02, doi:10.1029/2006GL026913.

Benson, B. B., and D. Krause (1984), The concentration and isotopic fractionation of oxygen dissolved in freshwater and seawater in equilibrium with the atmosphere, *Limnol. Oceanogr.*, *29*, 620–632, doi:10.4319/lo.1984.29.3.0620.

Bittig, H. C., B. Fiedler, T. Steinhoff, and A. Körtzinger (2012), A novel electrochemical calibration setup for oxygen sensors and its use for the stability assessment of Aanderaa optodes, *Limnol. Oceanogr. Methods*, *10*, 921–933, doi:10.4319/lom.2012.10.921.

Bittig, H. C., B. Fiedler, R. Scholz, G. Krahmann, and A. Körtzinger (2014), Time response of oxygen optodes on profiling platforms and its dependence on flow speed and temperature, *Limnol. Oceanogr. Methods*, *12*, 617–636, doi:10.4319/lom.2014.12.617.

Carlson, J. (2002), Development of an optimised dissolved oxygen sensor for oceanographic profiling, *Int. Ocean Syst.*, *6*, 20–21.

Clarke, R. A., and A. R. Coote (1988), The formation of Labrador Sea Water. Part III: The evolution of oxygen and nutrient concentration, *J. Phys. Oceanogr.*, *18*, 469–480, doi:10.1175/1520-0485(1988)018<0469:TFOLSW>2.0.CO;2.

Clarke, R. A., and J.-C. Gascard (1983), The formation of Labrador Sea Water. Part I: Large-scale processes, *J. Phys. Oceanogr.*, *13*, 1764–1778, doi:10.1175/1520-0485(1983)013<1764:TFOLSW>2.0.CO;2.

Curry, R. G., M. S. McCartney, and T. M. Joyce (1998), Oceanic transport of subpolar climate signals to mid-depth subtropical waters, *Nature*, *391*, 575–577, doi:10.1038/35356.

D'Asaro, E. A., and C. McNeil (2013), Calibration and stability of oxygen sensors on autonomous floats, *J. Atmos. Oceanic Technol.*, *30*, 1896–1906, doi:10.1175/JTECH-D-12-00222.1.

de Jong, M. F., A. S. Bower, and H. H. Furey (2016), Seasonal and interannual variations of Irminger ring formation and boundary-interior heat exchange in FLAME, *J. Phys. Oceanogr.*, *46*, 1717–1731, doi:10.1175/JPO-D-15-0124.1.

Dee, D. P., et al. (2011), The ERA-Interim reanalysis: Configuration and performance of the data assimilation system, *Q. J. R. Meteorol. Soc.*, *137*, 553–597, doi:10.1002/qj.828.

Dufresne, J.-L., et al. (2013), Climate change projections using the IPSL-CM5 Earth System Model: From CMIP3 to CMIP5, *Clim. Dyn.*, *40*, 2123–2165, doi:10.1007/s00382-012-1636-1.

Dunne, J. P., et al. (2013), GFDL's ESM2 global coupled climate-carbon Earth system models. Part II: Carbon system formulation and baseline simulation characteristics, *J. Clim.*, *26*, 2247–2267, doi:10.1175/JCLI-D-12-00150.1.

Emerson, S., and S. Bushinsky (2016), The role of bubbles during air-sea gas exchange, *J. Geophys. Res. Oceans*, *121*, 4360–4376, doi:10.1002/2016JC011744.

Garcia, H. E., and L. I. Gordon (1992), Oxygen solubility in seawater: Better fitting equations, *Limnol. Oceanogr.*, *37*, 1307–1312, doi:10.4319/lo.1992.37.6.1307.

Gruber, N., S. Doney, S. Emerson, D. Gilbert, T. Kobayashi, A. Körtzinger, G. C. Johnson, K. S. Johnson, S. C. Riser, and O. Ulloa (2010), Adding oxygen to Argo: Developing a global in-situ observatory for ocean deoxygenation and biogeochemistry, in *Proceedings of the "OceanObs'09: Sustained Ocean Observations and Information for Society" Conference*, vol. 2, ESA Publ. WPP-306, Venice, Italy, doi:10.5270/OceanObs09.cwp.39.

Harrison, W. G., and W. K. W. Li (2007), Phytoplankton growth and regulation in the Labrador Sea: Light and nutrient limitation, *J. Northwest Atlantic Fish. Sci.*, *39*, 71–82.

Harrison, W. G., K. Y. Børsheim, W. K. W. Li, G. L. Maillet, P. Pepin, E. Sakshaug, M. D. Skogen, and P. A. Yeats (2013), Phytoplankton production and growth regulation in the Subarctic North Atlantic: A comparative study of the Labrador Sea-Labrador/Newfoundland shelves and Barents/Norwegian/Greenland seas and shelves, *Prog. Oceanogr.*, *114*, 26–45, doi:10.1016/j.pocean.2013.05.003.

Hurrell, J. W., Y. Kushnir, G. Ottersen, and M. Visbeck (2013), An overview of the North Atlantic Oscillation, in *The North Atlantic Oscillation: Climatic Significance and Environmental Impact*, pp. 1–35, AGU, Washington, D. C., doi:10.1029/134GM01.

Ilyina, T., K. D. Six, J. Segschneider, E. Maier-Reimer, H. Li, and I. Núñez-Riboni (2013), Global ocean biogeochemistry model HAMOCC: Model architecture and performance as component of the MPI-Earth system model in different CMIP5 experimental realizations, *J. Adv. Model. Earth Syst.*, *5*, 287–315, doi:10.1029/2012MS000178.

Ito, T., M. J. Follows, and E. A. Boyle (2004), Is AOU a good measure of respiration in the oceans?, *Geophys. Res. Lett.*, *31*, L17305, doi:10.1029/2004GL020900.

Jackson, L. C., K. A. Peterson, C. D. Roberts, and R. A. Wood (2016), Recent slowing of Atlantic overturning circulation as a recovery from earlier strengthening, *Nat. Geosci.*, *9*(7), 518–522, doi:10.1038/ngeo2715.

Kalnay, E., et al. (1996), The NCEP/NCAR 40-Year reanalysis project, *Bull. Am. Meteorol. Soc.*, *77*, 437–471, doi:10.1175/1520-0477(1996)077<0437:TNYRP>2.0.CO;2.

Keeling, R. F. (1993), On the role of large bubbles in air-sea gas exchange and supersaturation in the ocean, *J. Mar. Res.*, *51*, 237–271, doi:10.1357/0022240933223800.

Keeling, R. F., A. Körtzinger, and N. Gruber (2010), Ocean deoxygenation in a warming world, *Ann. Rev. Mar. Sci.*, *2*, 199–229, doi:10.1146/annurev.marine.010908.163855.

Kihm, C., and A. Körtzinger (2010), Air-sea gas transfer velocity for oxygen derived from float data, *J. Geophys. Res. Oceans*, *115*, C12003, doi:10.1029/2009JC006077.

Körtzinger, A., J. I. Hedges, and P. D. Quay (2001), Redfield ratios revisited: Removing the biasing effect of anthropogenic CO_2, *Limnol. Oceanogr.*, *46*, 964–970, doi:10.4319/lo.2001.46.4.0964.

Körtzinger, A., J. Schimanski, U. Send, and D. W. R. Wallace (2004), The ocean takes a deep breath, *Science*, *306*, 1337–1337, doi:10.1126/science.1102557.

Körtzinger, A., U. Send, D. W. R. Wallace, J. Karstensen, and M. DeGrandpre (2008), Seasonal cycle of O_2 and pCO_2 in the central Labrador Sea: Atmospheric, biological, and physical implications, *Global Biogeochem. Cycles*, *22*, GB1014, doi:10.1029/2007GB003029.

Lazier, J. (1973), The renewal of Labrador Sea Water, *Deep Sea Res. Oceanogr. Abstr.*, *20*, 341–353, doi:10.1016/0011-7471(73)90058-2.

Levitus, S., et al. (2013), The World Ocean Database, *Data Sci. J.*, *12*, WDS229–WDS234, doi:10.2481/dsj.WDS-041.

Li, M., J. Liu, Z. Wang, H. Wang, Z. Zhang, L. Zhang, and Q. Yang (2013), Assessment of sea surface wind from NWP reanalyses and satellites in the Southern Ocean, *J. Atmos. Oceanic Technol.*, *30*, 1842–1853, doi:10.1175/JTECH-D-12-00240.1.

Liang, J.-H., C. Deutsch, J. C. McWilliams, B. Baschek, P. P. Sullivan, and D. Chiba (2013), Parameterizing bubble-mediated air-sea gas exchange and its effect on ocean ventilation, *Global Biogeochem. Cycles*, *27*, 894–905, doi:10.1002/gbc.20080.

Lilly, J., P. Rhines, F. Schott, K. Lavender, J. Lazier, U. Send, and E. D'Asaro (2003), Observations of the Labrador Sea eddy field, *Prog. Oceanogr.*, *59*, 75–176, doi:10.1016/j.pocean.2003.08.013.

Liss, P. S., and L. Merlivat (1986), Air-sea gas exchange rates: Introduction and synthesis, in *The Role of Air-Sea Exchange in Geochemical Cycling*, edited by P. Buat-Ménard, pp. 113–127, Springer, Netherlands, Dordrecht, doi:10.1007/978-94-009-4738-2_5.

Marshall, J., and F. Schott (1999), Open-ocean convection: Observations, theory, and models, *Rev. Geophys.*, *37*, 1–64, doi:10.1029/98RG02739.

McKinley, G. A., M. J. Follows, J. Marshall, and S.-M. Fan (2003), Interannual variability of air-sea O_2 fluxes and the determination of CO_2 sinks using atmospheric O_2/N_2, *Geophys. Res. Lett.*, *30*, 1101, doi:10.1029/2002GL016044.

Mesinger, F., et al. (2006), North American Regional Reanalysis, *Bull. Am. Meteorol. Soc.*, *87*(3), 343–360, doi:10.1175/BAMS-87-3-343.

Moore, G. W. K., R. S. Pickart, and I. A. Renfrew (2008), Buoy observations from the windiest location in the world ocean, Cape Farewell, Greenland, *Geophys. Res. Lett.*, *35*, L18802, doi:10.1029/2008GL034845.

Nightingale, P. D., G. Malin, C. S. Law, A. J. Watson, P. S. Liss, M. I. Liddicoat, J. Boutin, and R. C. Upstill-Goddard (2000), In situ evaluation of air-sea gas exchange parameterizations using novel conservative and volatile tracers, *Global Biogeochem. Cycles*, *14*, 373–387, doi:10.1029/1999GB900091.

Plant, J. N., K. S. Johnson, C. M. Sakamoto, H. W. Jannasch, L. J. Coletti, S. C. Riser, and D. D. Swift (2016), Net community production at Ocean Station Papa observed with nitrate and oxygen sensors on profiling floats, *Global Biogeochem. Cycles*, *30*, 859–879, doi:10.1002/2015GB005349.

Renfrew, I. A., G. N. Petersen, D. A. J. Sproson, G. W. K. Moore, H. Adiwidjaja, S. Zhang, and R. North (2009), A comparison of aircraft-based surface-layer observations over Denmark Strait and the Irminger Sea with meteorological analyses and QuikSCAT winds, *Q. J. R. Meteorol. Soc.*, *135*(645), 2046–2066, doi:10.1002/qj.444.

Schmidtko, S., L. Stramma, and M. Visbeck (2017), Decline in global oceanic oxygen content during the past five decades, *Nature*, *542*(7641), 335–339, doi:10.1038/nature21399.

Smith, G. C., F. Roy, P. Mann, F. Dupont, B. Brasnett, J.-F. Lemieux, S. Laroche, and S. Bélair (2014), A new atmospheric dataset for forcing ice-ocean models: Evaluation of reforecasts using the Canadian global deterministic prediction system, *Q. J. R. Meteorol. Soc.*, *140*, 881–894, doi:10.1002/qj.2194.

Stanley, R. H. R., W. J. Jenkins, D. E. Lott, and S. C. Doney (2009), Noble gas constraints on air-sea gas exchange and bubble fluxes, *J. Geophys. Res.*, *114*, C11020, doi:10.1029/2009JC005396.

Stendardo, I., and N. Gruber (2012), Oxygen trends over five decades in the North Atlantic, *J. Geophys. Res.*, *117*, C11026, doi:10.1029/2012JC007909.

Straneo, F. (2006), On the connection between dense water formation, overturning, and poleward heat transport in a convective Basin, *J. Phys. Oceanogr.*, *36*, 1822–1840, doi:10.1175/JPO2932.1.

Sweeney, C., E. Gloor, A. R. Jacobson, R. M. Key, G. McKinley, J. L. Sarmiento, and R. Wanninkhof (2007), Constraining global air-sea gas exchange for CO_2 with recent bomb ^{14}C measurements, *Global Biogeochem. Cycles*, *21*, GB2015, doi:10.1029/2006GB002784.

Takeshita, Y., T. R. Martz, K. S. Johnson, J. N. Plant, D. Gilbert, S. C. Riser, C. Neill, and B. Tilbrook (2013), A climatology-based quality control procedure for profiling float oxygen data, *J. Geophys. Res. Oceans*, *118*, 5640–5650, doi:10.1002/jgrc.20399.

Talley, L., and M. McCartney (1982), Distribution and circulation of Labrador Sea Water, *J. Phys. Oceanogr.*, *12*(11), 1189–1205, doi:10.1175/1520-0485(1982)012<1189:DACOLS>2.0.CO;2.

Taylor, K. E., R. J. Stouffer, and G. A. Meehl (2012), An overview of CMIP5 and the experiment design, *Bull. Am. Meteorol. Soc.*, *93*, 485–498, doi:10.1175/BAMS-D-11-00094.1.

Tengberg, A., et al. (2006), Evaluation of a lifetime-based optode to measure oxygen in aquatic systems, *Limnol. Oceanogr. Methods*, *4*, 7–17, doi:10.4319/lom.2006.4.7.

Thorpe, S. A. (1982), On the clouds of bubbles formed by breaking wind-waves in deep water, and their role in air-sea gas transfer, *Philos. Trans. R. Soc. London, Ser. A*, *304*, 155–210, doi:10.1098/rsta.1982.0011.

Tjiputra, J. F., K. Assmann, M. Bentsen, I. Bethke, O. H. Otterå, C. Sturm, and C. Heinze (2010), Bergen Earth system model (BCM-C): Model description and regional climate-carbon cycle feedbacks assessment, *Geosci. Model Dev.*, *3*, 123–141, doi:10.5194/gmd-3-123-2010.

Uchida, H., T. Kawano, I. Kaneko, and M. Fukasawa (2008), In situ calibration of optode-based oxygen sensors, *J. Atmos. Oceanic Technol.*, *25*, 2271–2281, doi:10.1175/2008JTECHO549.1.

Vagle, S., C. McNeil, and N. Steiner (2010), Upper ocean bubble measurements from the NE Pacific and estimates of their role in air-sea gas transfer of the weakly soluble gases nitrogen and oxygen, *J. Geophys. Res.*, *115*, C12054, doi:10.1029/2009JC005990.

Wallace, D. W. R., and C. D. Wirick (1992), Large air-sea gas fluxes associated with breaking waves, *Nature*, *356*, 694–696, doi:10.1038/356694a0.

Wanninkhof, R. (1992), Relationship between wind speed and gas exchange over the ocean, *J. Geophys. Res.*, *97*, 7373–7382, doi:10.1029/92JC00188.

Wanninkhof, R. (2014), Relationship between wind speed and gas exchange over the ocean revisited, *Limnol. Oceanogr. Methods*, *12*, 351–362, doi:10.4319/lom.2014.12.351.

Wanninkhof, R., and W. R. McGillis (1999), A cubic relationship between air-sea CO_2 exchange and wind speed, *Geophys. Res. Lett.*, *26*, 1889–1892, doi:10.1029/1999GL900363.

Wanninkhof, R., W. E. Asher, D. T. Ho, C. Sweeney, and W. R. McGillis (2009), Advances in quantifying air-sea gas exchange and environmental forcing, *Ann. Rev. Mar. Sci.*, *1*, 213–244, doi:10.1146/annurev.marine.010908.163742.

Weaver, A. J., et al. (2001), The UVic Earth System Climate Model: Model description, climatology, and applications to past, present and future climates, *Atmos. Ocean*, *39*, 361–428, doi:10.1080/07055900.2001.9649686.

Woolf, D. K. (1997), Bubbles and their role in gas exchange, in *The Sea Surface and Global Change*, edited by P. S. Liss and R. A. Duce, pp. 173–206, Cambridge Univ. Press, Cambridge, U. K., doi:10.1017/CBO9780511525025.007.

Woolf, D. K., and S. A. Thorpe (1991), Bubbles and the air-sea exchange of gases in near-saturation conditions, *J. Mar. Res.*, *49*, 435–466, doi:10.1357/002224091784995765.

Yashayaev, I., and J. Loder (2009), Enhanced production of Labrador Sea Water in 2008, *Geophys. Res. Letters*, *36*, L01606, doi:10.1029/2008GL036162.

Yashayaev, I., and J. W. Loder (2016), Recurrent replenishment of Labrador Sea Water and associated decadal-scale variability, *J. Geophys. Res. Oceans*, *121*, 8095–8114, doi:10.1002/2016JC012046.